Available online at www.sciencedirect.com
SCIENCE DIRECT®
International Journal of Mass Spectrometry 235 (2004) 83–89
International Journal of Mass Spectrometry
www.elsevier.com/locate/ijms

Ion chemistry in diethylzinc

C.Q. Jiao [a], C.A. DeJoseph Jr. [b], A. Garscadden [b,*]

[a] *Innovative Scientific Solutions Inc., Dayton, OH 45440-3638, USA*
[b] *Air Force Research Laboratory, Wright-Patterson AFB, OH 45433-7251, USA*

Received 6 April 2004; accepted 6 April 2004

Abstract

Electron impact ionization of diethylzinc has been measured by Fourier transform mass spectrometry. The ionization produces the parent ion $ZnC_4H_{10}^+$ and fragment ions including major metal-containing ions $ZnC_2H_5^+$ and Zn^+, as well as organic moiety ions, mainly $C_2H_5^+$. The total ionization cross-section reaches a maximum of 7.9×10^{-16} cm^2 at ~80 eV. Redistribution of the ion composition by ion–molecule reactions results in the ionic population being dominated by the final product ion $ZnC_8H_{17}^+$. Several dimer ions have been observed as the intermediate products in the ion–molecule reactions, but no larger Zn cluster ions have been detected. The argon ion charge-transfer reaction with diethylzinc generates mainly $ZnC_2H_5^+$ and $C_2H_5^+$.

Keywords: Diethylzinc; Electron collision; Ionization cross-section; Ion–molecule reaction

1. Introduction

Diethylzinc $Zn(C_2H_5)_2$ is used as a precursor gas for plasma-enhanced chemical vapor deposition (PECVD) to prepare thin films of ZnO [1,2], which is one of the more attractive materials for light-emitting devices due to its wide direct band gap and large excitonic binding energy [3].There have been several other techniques to prepare ZnO film including molecular beam epitaxy (MBE) [4,5], metalorganic chemical vapor deposition (MOCVD) [6], magnetron sputtering [7,8], and pulsed laser deposition [9,10]. The PECVD technique provides improved film quality by densification induced by plasma bombardment and ultraviolet irradiation. The presence of abundant radicals and ions also enhances the surface reactions. This paper presents our study on the formation of positive ions from $Zn(C_2H_5)_2$ by electron impact ionization and by subsequent ion–molecule reactions, with the goal of having a better understanding of the charged particle collisions in low pressure plasmas involving diethylzinc.

2. Experimental

All of the experiments are performed using a modified Extrel FTMS equipped with a cubic ion cyclotron resonance trapping cell (5 cm on a side) and a 2 T superconducting magnet [11]. The theory and methodology of FTMS have been well documented in the literature [12–14]. $Zn(C_2H_5)_2$ (95+%, Strem) is further processed by applying multiple liquid N_2 freeze–pump–thaw cycles to remove non-condensable gases. $Zn(C_2H_5)_2$ is mixed with Ar (99.999%, Matheson) with a ratio of about 1:1 to a total pressure of ~10 Torr, as determined by capacitance manometry. The mixture is then admitted through a precision leak valve into the FTMS system. Ions are formed by electron impact in the trapping cell at pressures in the 10^{-7} Torr range. An electron gun (Kimball Physics ELG2, Wilton, NH) irradiates the cell with a few hundred picocoulombs of low-energy electrons (detailed description of the electron beam is given below). The motion of the ions is constrained radially by the superconducting magnetic field and axially by an electrostatic potential (trapping potential) applied to the trap faces that are perpendicular to the magnetic field. The trapping potential is usually set to 10 V. Ions of all mass-to-charge ratio are simultaneously and coherently excited into cyclotron orbits using Stored Waveform Inverse Fourier

* Corresponding author. Tel.: +1-937-255-2246; fax: +1-937-656-4657.
E-mail address: alan.garscadden@wpafb.af.mil (A. Garscadden).

1387-3806/$ – see front matter © 2004 Published by Elsevier B.V.
doi:10.1016/j.ijms.2004.04.003

Transform (SWIFT) [15–17] applied to two opposing trap faces, which are parallel to the magnetic field. Following the cyclotron excitation, the image currents induced on the two remaining faces of the trap are amplified, digitized, and Fourier analyzed to yield a mass spectrum.

FTMS is an established technique for studying the kinetics of charged particle reactions, in which the signal peak heights are used to evaluate the number of ions in the cell [18]. In this study, the intensity ratios of the ions from $Zn(C_2H_5)_2$ to Ar give cross-sections relative to those for argon ionization [19] since the pressure ratio of $Zn(C_2H_5)_2$ to Ar is known.

To study the subsequent reactions of ions generated from electron impact ionization with their parent molecule, a mixture of $Zn(C_2H_5)_2$ and Ar with a ratio of ∼1:10 is used. An ion to be studied is selected by using SWIFT to eject other ions out of the trapping cell, followed by a cooling period in which the ion undergoes multiple collisions with Ar at a total pressure of 4.5×10^{-6} Torr for various times, typically 500 ms. SWIFT is used again to select the ion to be studied from others that are formed during the cooling period, followed by a programmed reaction time varying from 0 to 1000 ms. The cooling period can serve two purposes: (i) excited ions are thermalized by collisions with Ar atoms, and (ii) excited ions with reaction rates greater than the ground state ions are exhausted. The pressure of Ar and the length of the cooling period are adjusted so that at the end of the cooling period, there are still sufficient reactant ions to study and their reaction shows a single exponential decay to the end of the reaction time at which only a 3% or fewer of the reactant ions are left over. With an overwhelming Ar partial pressure, Ar^+ is overpopulated in the electron impact ionization, resulting in a significant space charge effect. To eliminate this effect, a single frequency rf is applied during the electron beam on period to continuously eject Ar^+ out of the trapping cell.

The trapping cell of the Extrel FTMS was modified by adding a pair of screen electrodes in front of the trapping plates. A significant improvement to the quality of the cross-section data has been achieved by this modification: holding the screens at ground potential produces the particle-in-a-box potential (rather than the harmonic oscillator potential) along the *z*-axis of the trapping cell [20]. Thus, it is possible to apply relatively high trapping potentials to trap more kinetically energetic ions, while in most of the volume of the cell, the potential drop is small enough to avoid the broadening of the electron energy distribution. Wang and Marshall [21] have a cell geometry similar to the one in our FTMS instrument and give a detailed description of the design of the screen electrodes. Each screen electrode was constructed from 0.0010 in. diameter tungsten 50 × 50 mesh (Unique Wire Weaving Co. Inc., Hillside, NJ); two out of every three wires were then removed to give a final mesh of 16/in. The mesh was held in place by spot-welds to a 314 stainless steel frame that was positioned 1/8 in. inside of the adjoining trapping plate. When the trapping potential is set to 10 V as mentioned above, the potential drop within the screen electrode region along the *z*-axis is estimated to be 0.3 V.

The Kimball Physics ELG-2 electron gun is rated for energies of 10–1000 eV with beam currents of 1 nA–3 μA. The filament has a radius of 0.04 cm and is 0.1 cm long. The electron beam has a Gaussian spatial distribution, and the energy spread of the beam is about 0.25 eV plus the space-charge well of the beam [22]. Combining the electron energy spread in the electron source and the potential drop in the trapping cell mentioned above, we estimate the uncertainty of the ionizing electron energies in the FTMS trapping cell to be ±0.6 eV. In the present experiments, only the formation of positive ions is studied and, therefore, cross-sections and other kinetic data reported in this paper refer to the positive ion production only.

3. Results and discussion

Electron impact ionization of $Zn(C_2H_5)_2$ produces a variety of ions including Zn-containing ions and the organic moiety ions, $C_2H_a^+$ (a = 1–6), $C_3H_b^+$ (b = 2–7), and $C_4H_c^+$ (c = 2, 3, 5–9). The ionization cross-sections as functions of the electron energy are shown in Fig. 1, for those ions that are formed readily, i.e., with the cross-sections greater than 10^{-18} cm^2 at 70 eV. The parent ion $ZnC_4H_{10}^+$ is the first ion to be formed at low energies. Above 16 eV, the fragment ion $ZnC_2H_5^+$ becomes more important. At energies below 23 eV, the above two metal-containing ions dominate the ion population. Among all of the organic moiety ions, $C_2H_5^+$ is the most abundant. This ion is likely to result from the simple cleavage of the Zn–C bond in the parent ion. The parent ion fragmentation results in the formation of a variety of ions containing three or four carbon atoms through C-atom rearrangement. Interestingly, no noticeable formation of ions containing a single carbon atom has been observed over the energy range up to 200 eV.

The total ionization cross-section reaches a maximum of $7.9 \pm 1.4 \times 10^{-16}$ cm^2 at ∼80 eV. At most of the energies studied, $ZnC_2H_5^+$ contributes more than 0.25 but less than 0.5 of the ion population. All of the channels making Zn-containing ions together sum to more than 2/3 of the total positive ion production. In summary, the formation of Zn-containing ions is efficient. It is likely that in a plasma, dissociative recombination of these ions produces Zn-containing radicals.

Subsequent reactions of several selected ions with the parent gas molecule have been studied. The three major organic moiety ions, $C_2H_3^+$, $C_2H_5^+$ and $C_3H_5^+$,

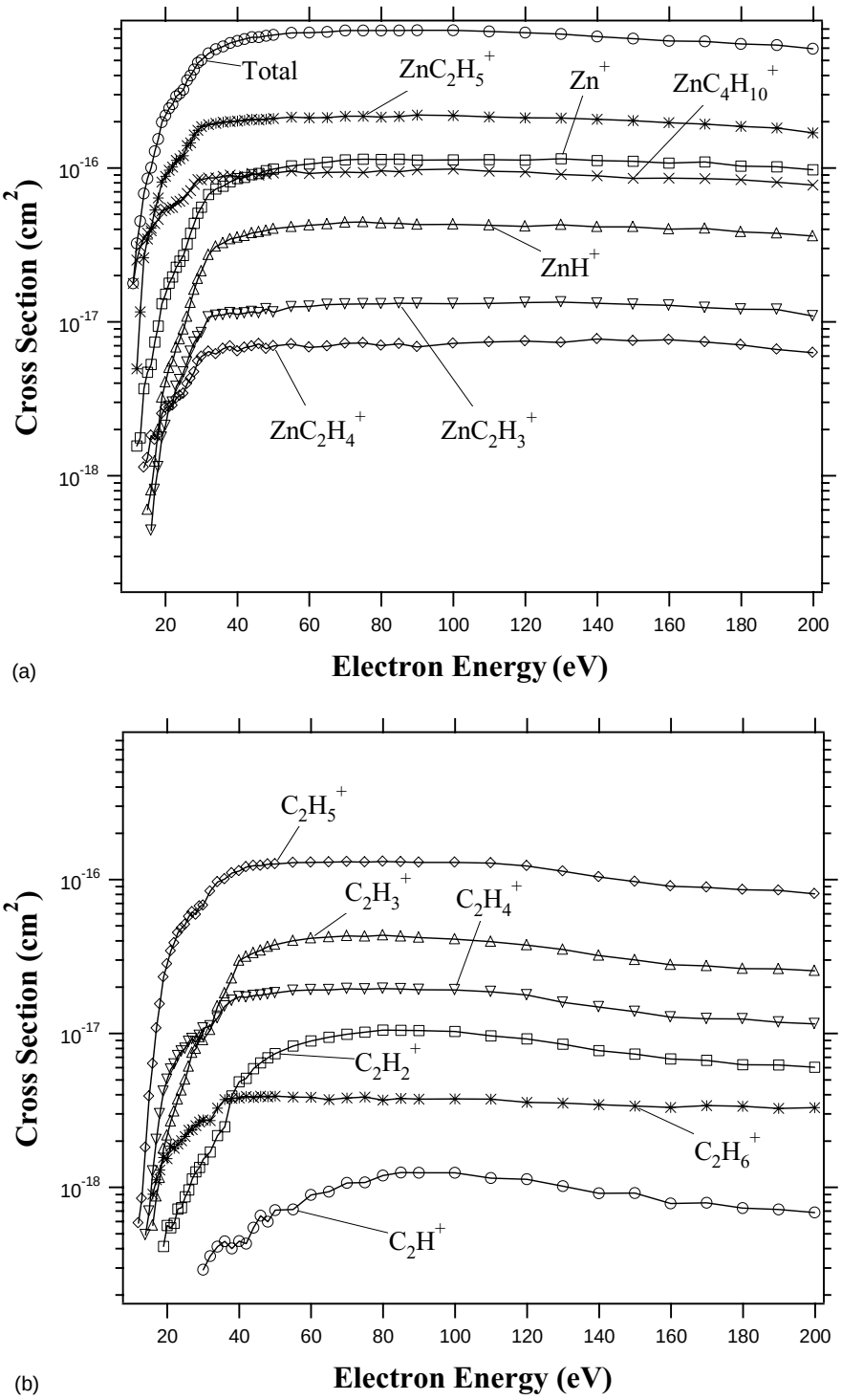

Fig. 1. Absolute cross-sections of electron impact ionization on diethylzinc. Combined with the uncertainty in the standard cross-section of Ar for calibration, the estimated uncertainty is ±18%. The lines through the data points act only as a guide to the eye. The fluctuations among the data points fall within experimental errors and therefore may have no physical meaning. (a) Total ionization cross-section of diethylzinc and partial ionization cross-sections for the production of the Zn-containing ions. (b) Partial ionization cross-sections of diethylzinc for the production of $C_2H_a^+$ ($a = 1$–6) ions. (c) Partial ionization cross-sections of diethylzinc for the production of $C_3H_b^+$ ($b = 2$–7) ions. (d) Partial ionization cross-sections of diethylzinc for the production of $C_4H_c^+$ ($c = 2$, 3 , 5–9) ions.

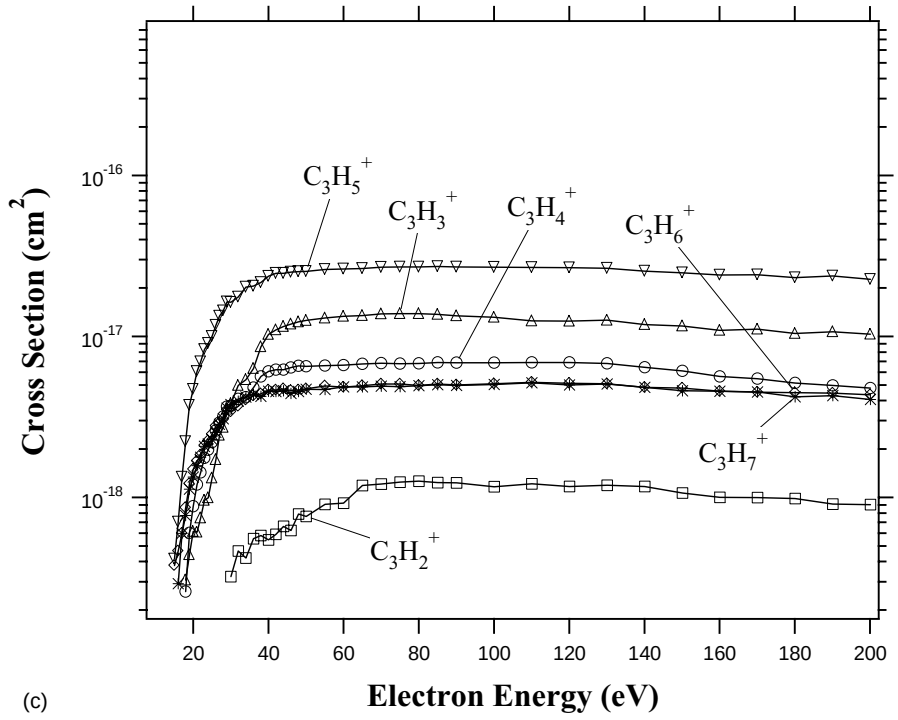

(c)

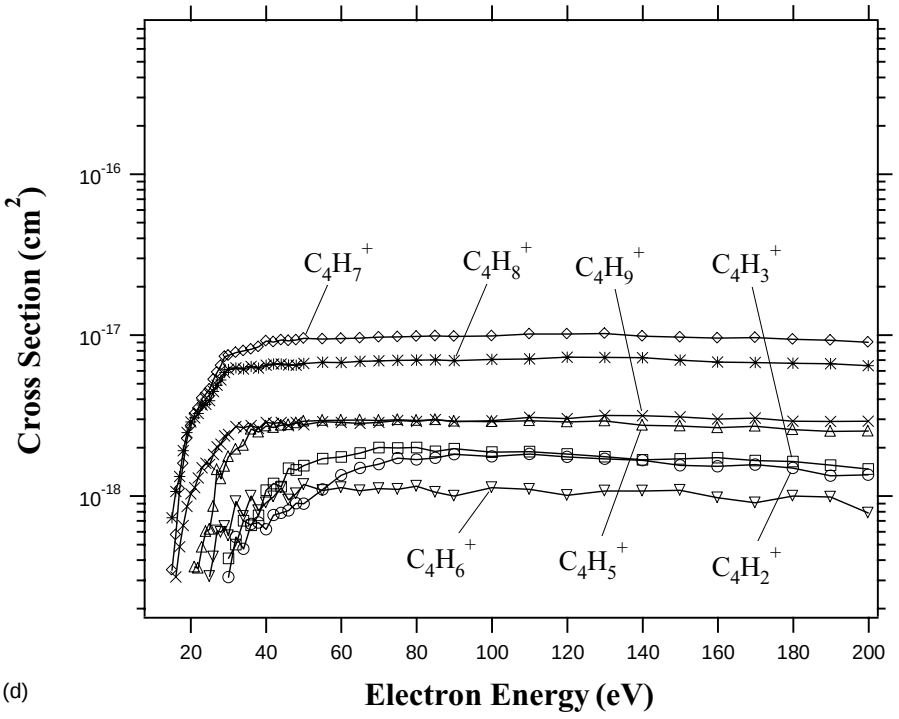

(d)

Fig. 1. (*Continued*).

are found to react with $Zn(C_2H_5)_2$ in a rather similar manner:

	$A^+ = C_2H_3^+$	$C_2H_5^+$	$C_3H_5^+$	
$A^+ + Zn(C_2H_5)_2$				
$\rightarrow ZnC_2H_5^+$	45%	57%	51%	(1)
$\rightarrow ZnC_4H_9^+$	39%	33%	39%	(2)
$\rightarrow ZnC_4H_{10}^+$	16%	10%	10%	(3)

In the above reactions, only the ionic products are shown, which are all Zn-containing ions. A^+ represents the three different reactant ions as shown above along with their respective branching ratios. The branching ratios reported in this paper have an estimated uncertainty of ±20%. We note that the branching ratio patterns for the reactions of the three reactant ions are analogous. Reaction (3) is a charge trans-

fer reaction and thus can give information on the upper limit of the ionization potential (IP) of $Zn(C_2H_5)_2$. For the case of the $C_2H_5^+$ reactant, there is no ambiguity in the structure and the IP is known. Therefore, reaction (3) gives the upper limit for the IP($Zn(C_2H_5)_2^+$) to be the value of the IP($C_2H_5^+$) that has been reported as 8.13 [23] or 8.34 eV. [24] in the literature. On the other hand, Creber and Bancroft [25] have reported a vertical IP of 8.6 eV for $Zn(C_2H_5)_2$. To address this discrepancy, we suggest that the adiabatic IP for $Zn(C_2H_5)_2$ is $\leq$8.34 eV and that the charge transfer reaction proceeds through a complex formation, allowing substantial rearrangement of the nuclei and subsequent electron transfer, and therefore relaxing Franck-Condon criteria as demonstrated by Chau and Bowers [26] for complex molecules. For similar thermochemical considerations, the neutral products of reactions (1) and (2) of $C_2H_5^+$ are proposed to be C_4H_{10} (butane) and C_2H_6 (ethane), respectively. Zn^+ is found to react with $Zn(C_2H_5)_2$ as shown below:

$$Zn^+ + Zn(C_2H_5)_2 \rightarrow ZnC_4H_{10}^+ + Zn \quad (85\%) \quad (4)$$
$$\rightarrow ZnC_2H_5^+ \text{ (Zn, 2C, 5H)} \quad (8\%) \quad (5)$$
$$\rightarrow Zn_2C_2H_5^+ + \text{(2C, 5H)} \quad (7\%) \quad (6)$$

Reaction (4) is a charge-transfer reaction, which is shown by the product isotope distribution; it retains the isotopic pattern of the neutral reactant: when ^{64}Zn is isolated and allowed to react with $Zn(C_2H_5)_2$, the product ion $ZnC_4H_{10}^+$ shows all of the Zn isotope natural abundance. This reaction proceeds efficiently, as expected given the thermochemistry discussed above for reaction (3). Reaction (5) displays a similar product isotope pattern, suggesting a charge transfer reaction or, more likely, an ethylide ($C_2H_5^-$) abstraction mechanism. Reaction (6) is a clustering reaction, with a relatively small probability. Buckner et al. [27] have studied formation and reactions of Zn_2^+ and found it to be a weakly bound cluster, with the Zn^+–Zn bond energy of only 0.56 ± 0.2 eV, compared to the Zn^+-alkyl bonds, such as Zn^+–CH_3 with the bond energy determined by Georgiadis and Armentrout [28] as 3.06 ± 0.14 eV. It may be reasonable to presume that the ionic cluster product in reaction (6), and other cluster products presented below, contain a Zn–Zn bond, which is weak and a displacement may occur when the ions are further reacted with $Zn(C_2H_5)_2$ as discussed later.

The reaction between $ZnC_2H_5^+$ and $Zn(C_2H_5)_2$, shown in reactions (7)–(9), produces $ZnC_4H_9^+$ as the major ionic product, which is absent in the electron impact ionization products.

$$ZnC_2H_5^+ + Zn(C_2H_5)_2$$
$$\rightarrow ZnC_4H_9^+ + \text{(Zn, 2C, 6H)} \quad (55\%) \quad (7)$$
$$\rightarrow Zn_2C_6H_{15}^+ \quad (24\%) \quad (8)$$
$$\rightarrow Zn_2C_4H_{11}^+ + \text{(2C, 4H)} \quad (21\%) \quad (9)$$

The product's isotopic pattern in reaction (7) is different from the Zn^+ reaction mentioned above (reaction (4)). When $^{64}ZnC_2H_5^+$ is isolated and reacted with $Zn(C_2H_5)_2$, the product ion $ZnC_4H_9^+$ has a isotope content that is made by mixing pure ^{64}Zn and the natural abundance of Zn in a ratio of approximately 1:1. To explain this product isotopic pattern, we propose that in the reaction, an intermediate complex between $ZnC_2H_5^+$ and $Zn(C_2H_5)_2$ is formed and that it undergoes some rearrangements that scramble the two Zn atoms, respectively, coming from the ionic and neutral reactants. It is noteworthy to point out that Zn isotope scrambling occurs between the reactants $ZnC_2H_5^+$ and $Zn(C_2H_5)_2$, probably via a symmetric reaction, i.e., a ethylide transfer reaction, yielding a shift in the isotopic pattern of the reactant ion as well as the product ion as a function of the reaction time. For this reason, we sample the product's isotopic pattern at a relatively early reaction time. This constraint applies to the similar reaction measurements discussed below. Reactions (8) and (9) produce two Zn-dimer ions. It is interesting that reaction (8) is a condensation reaction and that its probability is quite large, possibly facilitated by internal excitation to satisfy energy conservation.

$ZnC_4H_{10}^+$ reaction with $Zn(C_2H_5)_2$ generates the clustering ion $Zn_2C_6H_{15}^+$ as the major product:

$$ZnC_4H_{10}^+ + Zn(C_2H_5)_2$$
$$\rightarrow Zn_2C_6H_{15}^+ + \text{(2C, 5H)} \quad (78\%) \quad (10)$$
$$\rightarrow ZnC_8H_{17}^+ + \text{(Zn, 3H)} \quad (18\%) \quad (11)$$
$$\rightarrow Zn_2C_4H_{11}^+ + \text{(4C, 9H)} \quad (4\%) \quad (12)$$

In reaction (11), the product ion $ZnC_8H_{17}^+$ retains the isotope pattern of the ionic reactant, implying that the reaction may proceed via a complex formation followed by C-atom rearrangements, and when the complex breaks apart, the Zn atom originally from the reactant ion remains in the product ion. It is interesting to note that reactions (10)–(12) each produces high-energy radicals. These reactions proceed efficiently probably because the reactant ion is already an unstable odd-electron ion (radical ion). As Zn is primarily divalent, in some product ions such as $ZnC_8H_{17}^+$ ligands must have undergone coupling to form a larger ligand, such as in Zn^+–$C_8H_{17}^+$, for example.

The product ion $ZnC_4H_9^+$ from reaction (2) or (7) is found to react with $Zn(C_2H_5)_2$ as shown below:

$$ZnC_4H_9^+ + Zn(C_2H_5)_2$$
$$\rightarrow Zn_2C_6H_{15}^+ + \text{(2C, 4H)} \quad (69\%) \quad (13)$$
$$\rightarrow ZnC_8H_{17}^+ + \text{(Zn, 2H)} \quad (20\%) \quad (14)$$
$$\rightarrow Zn_2C_4H_{11}^+ + \text{(4C, 8H)} \quad (11\%) \quad (15)$$

The product's isotopic pattern in reaction (14) is similar to that in reaction (7) discussed above, with approximately equal contribution from the ionic and neutral reactants.

The two Zn-dimer ions, $Zn_2C_4H_{11}^+$ and $Zn_2C_6H_{15}^+$, which are generated from some of the above reactions undergo further reactions with $Zn(C_2H_5)_2$, respectively,

$$Zn_2C_4H_{11}^+ + Zn(C_2H_5)_2$$
$$\rightarrow ZnC_8H_{17}^+ + \text{(2Zn, 4H)} \quad (54\%) \quad (16)$$
$$\rightarrow Zn_2C_6H_{15}^+ + \text{(Zn, 2C, 3H)} \quad (46\%) \quad (17)$$
$$Zn_2C_6H_{15}^+ + Zn(C_2H_5)_2$$
$$\rightarrow ZnC_8H_{17}^+ + \text{(2Zn, 2C, 8H)} \quad (100\%) \quad (18)$$

Table 1
Relative rates of the ion–molecule reactions between selected ions and diethylzinc, and their relative reaction efficiencies, defined as ratios of the observed reaction rates over the calculated collision rates, assuming that Ar^+ reaction efficiency is unity

Reaction	Relative rate	Relative reaction efficiency
$Ar^+ + Zn(C_2H_5)_2$	1.0	1.0
$C_2H_3^+ + Zn(C_2H_5)_2$	1.1	0.94
$C_2H_5^+ + Zn(C_2H_5)_2$	0.82	0.72
$C_3H_5^+ + Zn(C_2H_5)_2$	0.67	0.68
$Zn^+ + Zn(C_2H_5)_2$	0.60	0.71
$ZnC_2H_5^+ + Zn(C_2H_5)_2$	0.49	0.64
$ZnC_4H_9^+ + Zn(C_2H_5)_2$	0.46	0.65
$ZnC_4H_{10}^+ + Zn(C_2H_5)_2$	0.52	0.74
$Zn_2C_4H_{11}^+ + Zn(C_2H_5)_2$	0.10	0.16
$Zn_2C_6H_{15}^+ + Zn(C_2H_5)_2$	0.050	0.08

The estimated uncertainty in the data is ±15%.

The product ion $ZnC_8H_{17}^+$ in reaction (18) retains the ionic reactant isotopic pattern, suggesting that one of the two Zn atoms in the reacting $Zn_2C_6H_{15}^+$ remains in the product ion. The reactions of the dimer ion $Zn_2C_2H_5^+$ that is generated from reaction (6) is not studied because of its low intensity not permitting a quantitative measurement.

$ZnC_8H_{17}^+$ is isolated and allowed to collide with $Zn(C_2H_5)_2$, but no obvious reaction has been observed. In summary, from the overall reactions presented above, we conclude that $ZnC_8H_{17}^+$ is the final product of the ion–molecule reactions in $Zn(C_2H_5)_2$. Ionic polymerization reactions produce several Zn-dimer ions but no larger cluster ions. The dimer ions in turn react with the parent gas molecule, eventually producing a single Zn-atom-containing ion.

Ar^+ reacts with $Zn(C_2H_5)_2$ to generate organic moiety ions as well as Zn-containing ions: $ZnC_2H_5^+$ (32%), $C_2H_5^+$ (28%), $C_2H_3^+$ (9%), Zn^+ (4%), ZnH^+ (3%), $ZnC_4H_{10}^+$ (3%), $ZnC_4H_9^+$ (1%), and $C_4H_7^+$ (1%). A comparison of the reaction rates of ions mentioned above to that of Ar^+ is shown in Table 1. Also shown in the table are the relative reaction efficiencies defined as the ratios of the observed reaction rates over the calculated collision rates, assuming that Ar^+ reaction efficiency is unity. The polarizability of $Zn(C_2H_5)_2$ and therefore its collision rate is not known, but the relative reaction efficiencies can be calculated using the following equation:

$$\text{relative reaction efficiency} = \text{relative rate} \times \sqrt{\frac{\mu_{x,\text{DEZn}}}{\mu_{\text{Ar,DEZn}}}}$$

where μ is the reduced mass of the ion and diethylzinc (DEZn):

$$\mu_{a,b} = \frac{m_a m_b}{(m_a + m_b)}.$$

From Table 1, we note that the reactions of the two Zn-dimer ions are significantly slower compared to the others.

4. Summary

Electron impact ionization of $Zn(C_2H_5)_2$ produces parent ion $ZnC_4H_{10}^+$ and fragment ions including metal-containing ions such as $ZnC_2H_5^+$ and Zn^+, as well as the organic moiety ions, mainly $C_2H_5^+$. At low electron energies (<23 eV), $ZnC_4H_{10}^+$ and $ZnC_2H_5^+$ dominate the ion population. The total ionization cross-section reaches a maximum of 7.9×10^{-16} cm^2 at ∼80 eV. More than 2/3 of the total cross-section belongs to Zn-containing ion production over most of the 10–200 eV electron energies studied. In the ion–molecule reactions, we find that the major organic moiety ions react with the parent gas forming Zn-containing ions, and the Zn-containing ions that are generated from the electron impact ionization or from the ion–molecule reactions react with the parent gas to produce heavier ions including Zn-dimer ions. No cluster ions larger than dimers have been found in the ion–molecule reactions studied. Most of the product ions from the reactions mentioned above are intermediate products; they react further with the parent gas to form a final product ion $ZnC_8H_{17}^+$.

Acknowledgements

The authors thank the Air Force Office of Scientific Research for support. We also appreciate helpful guiding comments of the referees.

References

[1] K. Haga, M. Kamidaira, Y. Kashiwaba, T. Sekiguchi, H. Watanabe, J. Crystal Growth 214/215 (2000) 77.
[2] B.S. Li, Y.C. Liu, Z.S. Chu, D.Z. Shen, Y.M. Lu, J.Y. Zhang, X.W. Fan, J. Appl. Phys. 91 (2002) 501.
[3] A. Shimizu, M. Kanbara, M. Hada, M. Kasuga, Jpn. J. Appl. Phys. 17 (1978) 1435.
[4] D.M. Bagnall, Y.F. Chen, Z. Zhu, T. Yao, M.Y. Shen, T. Goto, Appl. Phys. Lett. 73 (1998) 1038.
[5] F. Siah, Z. Yang, Z.K. Tang, G.K.L. Wong, M. Kawasaki, A. Ohtomo, H. Koinuma, Y. Segawa, J. Appl. Phys. 88 (2000) 2480.
[6] K. Haga, F. Katahira, H. Watanabe, Thin Solid Films 343/344 (1999) 145.
[7] A. Hachigo, H. Nakahata, K. Higaki, S. Fujii, S. Shikata, Appl. Phys. Lett. 65 (1994) 2556.
[8] J. Hinze, K. Ellmer, J. Appl. Phys. 88 (2000) 2443.
[9] S.V. Prasad, S.D. Walck, J.S. Zabinski, Thin Solid Films 360 (2000) 107.
[10] X.W. Sun, H.S. Kowk, J. Appl. Phys. 86 (1999) 408.
[11] P.D. Haaland, Chem. Phys. Lett. 170 (1990) 146.
[12] M.B. Comisarow, A.G. Marshall, Chem. Phys. Lett. 25 (1974) 282.
[13] A.G. Marshall, P.B. Grosshans, Anal. Chem. 63 (1991) 215A.
[14] Z. Liang, A.G. Marshall, Anal. Chem. 62 (1990) 70.
[15] A.G. Marshall, T.L. Wang, T.L. Ricca, J. Am. Chem. Soc. 107 (1985) 7983.
[16] S.J. Guan, Chem. Phys. 91 (1989) 775.
[17] L. Chen, A.G. Marshall, Int. J. Mass Spectrom. Ion Processes 79 (1987) 115.
[18] D.L. Rempel, S.K. Huang, M.L. Gross, Int. J. Mass Spectrom. Ion Processes 70 (1986) 163.

[19] H.C. Straub, P. Renault, B.G. Lindsay, K.A. Smith, R.F. Stebbings, Phys. Rev. A 52 (1995) 1115.
[20] S. Guan, A.G. Marshall, Int. J. Mass Spectrom. Ion Processes 146/147 (1995) 261.
[21] M. Wang, A.G. Marshall, Anal. Chem. 61 (1989) 1288.
[22] Kimball Physics, Inc., Wilton, New Hamshire. ELG-2A Electron Gun Instruction Manual, 1986.
[23] S.G. Lias, J.E. Bartmess, J.F. Liebman, J.L. Holmes, R.D. Levin, W.G. Mallard, J. Phys. Chem. Ref. Data, 17 (1988).
[24] H.M. Rosenstock, K. Draxl, B.W. Steiner, J.T. Herron, J. Phys. Chem. Ref. Data, 6 (1977).
[25] D.K. Creber, G.M. Bancroft, Inorg. Chem. 19 (1980) 643.
[26] M. Chau, M.T. Bowers, Int. J. Mass Spectrom. Ion Phys. 24 (1977) 191.
[27] S.W. Buckner, J.R. Gord, B.S. Freiser, J. Chem. Phys. 88 (1988) 3678.
[28] Georgiadis, P. B. Armentrout, J. Am. Chem. Soc. 108 (1986) 2119.